

THE PENNSYLVANIA STATE UNIVERSITY  
SCHREYER HONORS COLLEGE

DEPARTMENT OF CHEMISTRY

INVESTIGATION OF THE STATE OF WATER ADJACENT TO SOLID SURFACES  
USING DEUTERIUM NMR SPECTROSCOPY

SASHA HANAN SLIPAK

Spring 2010

A thesis  
submitted in partial fulfillment  
of the requirements  
for baccalaureate degrees  
in Chemistry and Mathematics  
with honors in Chemistry

Reviewed and approved\* by the following:

Alan J. Benesi  
Director of the NMR Facility and Lecturer in Chemistry  
Thesis Supervisor

Przemyslaw Maslak  
Associate Professor of Chemistry  
Honors Adviser

James B. Anderson  
Evan Pugh Professor of Chemistry

\* Signatures are on file in the Schreyer Honors College.

## ABSTRACT

The state of water adjacent to solid surfaces in freeze-dried starch and cellulose has been investigated using  $^2\text{H}$  NMR techniques. Quadrupole echo spectra of all samples at room temperature include a sharp central peak that corresponds to  $^2\text{H}_2\text{O}$ . Both compounds also showed additional powder patterns that have been attributed to rigid glucose O- $^2\text{H}$  groups. At lower temperatures ( $\leq -50^\circ\text{C}$ ), the central peak became irresolvable due to transition into the intermediate and slow exchange regime.  $T_1$  values spanning a range of temperatures obtained at two different magnetic fields closely match previous values for theoretical calculations that assumed fast tetrahedral jumps in a solid-state lattice. These low values suggest that the rate of motion is comparable to the Larmor frequency. Movement at this frequency ( $\sim 10^7$  Hz) is typically only seen in solids. The findings are consistent with previous data for a variety of porous silicates, which could not be matched with isotropic rotational diffusion models for liquid state  $^2\text{H}_2\text{O}$ . The sharp central peak at higher temperatures exhibited spin-lattice relaxation times of almost two orders of magnitude shorter than those of bulk  $^2\text{H}_2\text{O}$ , and exhibited magnetic field dependence, with  $T_1$  values at room temperature of 5.59 ms at 7.02 T and 9.67 ms at 11.75 T for starch, and 6.31 ms at 7.02 T and 10.6 ms at 11.75 T for cellulose. This data supports a hypothesis for solid-state water within the lattice structures of both starch and cellulose at room temperature and above.

# TABLE OF CONTENTS

Abstract .....	i
Table of Contents .....	ii
Acknowledgments .....	iv
<b>Chapter 1</b> Introduction to NMR Theory	
1.1 <b>NMR</b> .....	1
1.2 Quadrupolar Nuclei .....	2
1.3 Deuterium NMR .....	4
1.4 Quadrupolar Echo Experiments .....	5
1.5 Spin-Lattice Relaxation ( $T_1$ ) .....	5
1.6 $T_1$ Inversion Recovery Experiment .....	6
1.7 Molecular Motion and $T_1$ .....	8
1.8 $T_1$ Quadrupole Echo Experiment .....	9
1.9 Powder Patterns and Lineshape Analysis .....	10
<b>Chapter 2</b> Water	
2.1 <b>Water</b> .....	13
2.2 The Definition of Solid State .....	14
2.3 Solid State Tetrahedral Jumps and Bjerrum Defects .....	14
2.4 $C_2$ Jumps .....	15
<b>Chapter 3</b> Previous Research	
3.1 <b>Previous Studies</b> .....	16
3.2 Liquid State Isotropic Model vs. Solid State High Symmetry Model.....	17
<b>Chapter 4</b> Starch and Cellulose	

4.1	<b>Introduction</b>	19
4.2	Experimental	22
4.2.1	Sample Preparation	22
4.2.2	NMR Measurements	23
4.3	Results and Discussion	24
4.3.1	Quadrupole Echo Spectral Results	24
4.3.2	$T_1$ Inversion Recovery Results	27
4.4	Conclusions and Future Research	29
	References	31

## ACKNOWLEDGEMENTS

First and foremost I would like to thank Dr. Alan J. Benesi for giving me the opportunity to dive head first into chemistry. As his student, he instilled a love for the field and inspired me to pursue research in the very thing that he loved most about it—NMR. Through the years, he has taught me a great deal and has remained patient with me as I learned the techniques and concepts. He is always willing and eager to sit down and explain anything to me. It has truly been an honor to work with Dr. Benesi over these last two and a half years.

I would also like to thank my lab partner Shoshanna Pokras for her help in the completion of this thesis. Our relationship began with her teaching me how to run my first proton NMR and remained somewhat professional until our summer doing research together. Now I think of her as one of my good friends and whether we are competing about grades or discussing NMR over breakfast, we are always having a good time. I know that she will become an incredible chemist one day and finally prove to me which one of us is better.

The completion of this thesis would also have not been possible without the constant love and support from my family. My brother, Alan Slipak, (who himself endured the trials of an honors thesis) constantly encouraged me and pushed me to work harder. He constantly checked on my progress and attempted to keep me on track. Over the years he has been my biggest rival and we are constantly competing in everything. Nevertheless, he is one of my best friends and the greatest brother anyone could ask for. I love him. My parents, Vita and Peter Slipak, were also crucial in this journey. They supported me whenever I lost faith in my abilities and assured me that I could finish what

I started. I owe a large portion of my academic success to the values and attitudes they instilled into me as a child. They raised me to take pride in my work and taught me to do everything to the best of my abilities. They are truly wonderful parents and I love them both dearly.

I would also like to thank all of my friends who have helped me along the way. My roommates, in particular, have been with me since high school and I can always count on them to cheer me up. Whether we're having a debate on apartment policy or an intimate conversation they always seem to put me in good spirits (or at least leave me with a good story to tell). Peter Taylor has been on the receiving end of many of my frustrated rants and has always humored me and brought me back to earth. We have been inseparable since the 6<sup>th</sup> grade (barring some rough patches) and will hopefully stay close for a long time. He is not only my best friend, but is like a second brother to me and is truly amazing. Roma Amin, who I have only known for a short period of time, has also been wonderful. She was always willing and eager to keep me company late into the night and help me manage all of my responsibilities. She is an amazing friend and I consider myself blessed to know her. I would also like to thank Paul Munson, who not only reviewed my thesis but has also been a great TA and laser chess opponent. Through the hours I've spent playing him, I have learned a lot and gotten to take my mind off of academics and relax a bit. Although he is my TA, I think of him more as a friend.

I would also like to thank Tiffany Smith for her role in the completion of my thesis. She and I have gone through some rough times together, but in the end she was the one who pushed me to join the honors college in the first place, and for that I thank her. Although she wasn't around for the writing process, I somehow know she was

always there, supporting me. She has a way of always inspiring me and encouraging me to push forward. She can cheer me up in a matter of seconds and always accepts me for who I am. Tiffany is my best friend and I truly love her.

I would like to thank Dr. Pshemak Maslak and Dr. James Anderson for their contribution to my thesis. Dr. Maslak has advised me well over the years and has given me some great advice and tried to keep me on time with my future plans. He has been a great teacher and advisor over the years and I want to thank him for taking time out to review my thesis and serve on my defense board. I would also like to thank Dr. Anderson for being an amazing professor and agreeing to be a member of my defense committee.

Finally I would like to thank Dr. Bernie O'Hare, Tanuj Motwani, Dr. Anantheswaran, and Wenbin Luo for their help with the development and facilitation of this project. I would like also to thank The Pennsylvania State University for general support.

## CHAPTER ONE

### INTRODUCTION TO NMR THEORY

#### 1.1 NMR

Nuclear magnetic resonance, or NMR, is the most powerful analytical tool available to modern chemists. NMR can be utilized to accomplish a variety of tasks which previously were thought to be impossible. Not only can it determine the structure of compounds ranging from small organic molecules to proteins larger than 40 kDa, but it can also investigate the dynamics of both solids and liquids at a molecular level. One of NMR's best known yet least credited applications is its use in imaging biological systems, which can be accomplished with gradients of known strength and direction. This, of course, is known as magnetic resonance imaging, or more commonly, MRI.

The phenomenon of NMR was first discovered in 1938 by Isidor Rabi through his study of molecular beams. He found that once the resonant frequency for a given sample was reached, the beam intensity would reach a minimum.<sup>1</sup> The intensity would of course return if the frequency was increased or decreased from this resonance point. However, molecular beam studies proved to be difficult and inaccurate, resulting in the proposition that radio frequency methods should be used to detect nuclear moment reorientation. It was not until 1946 that the technique began to be refined through the work of Felix Bloch and Edward Purcell.<sup>2,3</sup>

NMR is an exceptionally practical analytical tool for many reasons. First and foremost, NMR is a non-destructive technique, meaning that the sample may be retrieved unaltered after the experiment is conducted. This property becomes extremely useful when little sample is available for analysis. The non-destructive nature of the technique is of course inherent in the



experimentation, as the samples are analyzed using radio waves, which are of relatively low energy and are passed through our bodies daily.

Although NMR is dependent upon several quantum mechanical principles, it may be rudimentarily explained using a classical approach. First of all, in order for an atom to be NMR active, it must fulfill certain requirements, the most important of which pertains to the number of nucleons in the atom. Nucleons (protons and neutrons), like all fermions, have an intrinsic half-integer spin ( $\pm \frac{1}{2}$ ). Any nuclei that have an odd number of protons and/or neutrons will have a net nuclear spin  $\geq \frac{1}{2}$ , resulting in a magnetic dipole moment,  $\mu$ , and rendering them NMR active. Fortunately, every element has at least one NMR active isotope. When an external magnetic field is applied to such nuclei, the magnetic dipole moment interacts with an applied magnetic field resulting in a separation in energy of the normally degenerate spin states. The individual nuclei exist in a superposition of these spin states. For the ensemble of nuclei, this yields a net magnetization vector aligned with  $\mathbf{B}_0$ . NMR collects information from the system by exciting the nuclei using nucleus-specific radio-frequency pulses which perturb the equilibrium populations of the spin states. As the nuclei relax back to equilibrium, they emit slightly different radio-frequency waves based on their specific chemical environments, allowing the detector to differentiate between different nuclei.

## 1.2 Quadrupolar Nuclei

While many of the most commonly used NMR active nuclei ( $^1\text{H}$ ,  $^{13}\text{C}$ ,  $^{15}\text{N}$ ,  $^{31}\text{P}$ , etc.) have a spin of  $I = \frac{1}{2}$ , the overall majority of NMR active nuclei have a spin of  $I \geq 1$ . Nuclei with  $I \geq 1$  possess a non-uniform distribution of positive charge in the nucleus, creating an electric quadrupole moment. The significance of this quadrupole moment is made apparent through its coupling interactions with inhomogeneous electric fields caused by other charges within the

system, resulting primarily from electron orbitals, which are collectively known as the electric field gradient, or EFG. This coupling is termed a quadrupolar interaction and is described by the quadrupolar coupling constant (qcc). This constant is directly proportional to the electric field gradient at the nuclear site and can be calculated from the electronic ground state electron density. The EFG is generated by electrons and nuclei in the immediate vicinity of the nucleus. Unless the nucleus experiences a chemical reaction that changes the EFG, this yields a single quadrupole coupling tensor for the nucleus. This makes it possible to analyze the system as a whole and not have to worry about microenvironments which might cause deviation of this constant.

Although quadrupolar interactions are present in all physical states of matter, in NMR they are less influential in their effects on the NMR spectrum for gaseous and liquid samples. Although often not visible in the NMR spectrum, quadrupolar interactions still have a profound effect on NMR relaxation for liquids and gases. It is the rapid molecular motion in these states which results in the dynamic averaging of the EFG.

In solids, however, quadrupolar interactions are dominant and easily observable in the spectrum. NMR relaxation and the solid state spectrum itself are significantly affected by the specific angular motions of the EFG. Solid state NMR, as used by this investigation, can take advantage of the strength of these interactions to study the molecular dynamics of various systems. In fact, the quadrupolar interactions are often large enough to completely dictate the spectrum resulting from solid samples, allowing for the neglect of other interactions, including dipole-dipole and chemical shift.<sup>4</sup> Aside from these interactions, paramagnetic interactions can also be significantly large; however, these interactions can be avoided by using substances without paramagnetic impurities.<sup>5</sup>

### 1.3 Deuterium NMR

Deuterium, one of three isotopes of hydrogen, is an extraordinarily useful quadrupolar nucleus. Conveniently, it can replace hydrogen without perturbing a given system and can easily be monitored using a variety of NMR techniques, including solid state NMR. Despite this convenience, there are certain properties of the deuterium nucleus that must be considered. Deuterium has nuclear spin  $I = 1$ , and consequently possesses a quadrupole moment and, as described above, participates in coupling interactions with the EFG. As a result of these interactions, the magnetic energy levels are disturbed and cause the solid state  $^2\text{H}$  resonance to broaden to as much as 400 kHz. Luckily, modern day NMR instrumentation allows for the observation of undistorted spectra over such a large spectral width. In addition to the aforementioned properties, the nuclear spin of  $I=1$  means that the deuterium nucleus has only two spectral transitions. This is of particular use, as it greatly reduces the complexity of NMR spectra in contrast to higher spin nuclei.

The quadrupolar interactions of the nucleus do more than just alter energy levels. As previous studies have shown, when molecularly incorporated (in this case  $\text{D}_2\text{O}$ ), these interactions directly link deuterium spectral frequencies with the orientation of the covalent bond relative to the nucleus. The covalent bond is parallel to the principal axis of the electric field gradient tensor. Because of this, quadrupole dependent experiments (to be later discussed) can be used to quantify molecular dynamics when performed in conjunction with relaxation experiments. The experiments may be used to describe molecular motion spanning a range of frequencies from the order of nanoseconds to seconds. As a result of this, a large portion of  $^2\text{H}$  solid state NMR is focused on the investigation of molecular motion, and yet it is still used in a variety of applications including structure determination.<sup>4,6</sup>

## 1.4 **Quadrupolar Echo Experiments**

As a result of the wide frequency range of the spectrum and the rapid decay of the signal, the standard single pulse and acquisition sequence, typically used in liquid state NMR, cannot be used in deuterium NMR. Instead, an echo is required to allow for the signal to be detected and to prevent extreme lineshape distortion resulting from pulse breakthrough of the FID (free induction decay). These experiments, known as quadrupole echo experiments, utilize a  $90_x^\circ$ - $\tau$ - $90_y^\circ$  pulse sequence. The sample is first hit with a  $90_x^\circ$  pulse, followed by a variable delay,  $\tau$ , and then a  $90_y^\circ$  pulse to finish the sequence. After another delay,  $\tau$ , the data acquisition begins. The previously mentioned signal decay is caused by the random arrangement of molecules in the solid sample. The frequencies at which these nuclei emit destructively interfere, causing a rapid decrease in signal intensity. This could be overcome if the signal were captured immediately after the initial  $90^\circ$  pulse. Unfortunately, due to the limitations of the electronics involved, a delay is required before signal acquisition. To compensate for this, the second pulse is used to form an “echo”, which refocuses the magnetization, imitating the signal intensity after the initial pulse. The signal is captured halfway through the echo at which point the signal is at its maximum.

## 1.5 **Spin-Lattice Relaxation ( $T_1$ )**

Upon exposure to a magnetic field, the magnetic dipole moment of each nucleus in a given sample aligns itself in such a way that the net magnetization of the sample matches the direction of the external magnetic field,  $\mathbf{B}_0$ . In fact, the magnetic dipole moment of each individual nucleus exists in a superposition of the allowed quantum states (three in the case of deuterium), which correspond to the Zeeman energy levels of the nucleus.<sup>7</sup> The levels form as a result of a break in degeneracy and subsequent modification in energy caused by the external

magnetic field. The energy difference between the allowed states is given by **Equation 1** below. Immediately after placing a sample in a magnetic field, the population of each state is essentially equal. However, this configuration is not ideal and the system will eventually relax to reach the lowest state possible, as described by the Boltzmann distribution between adjacent energy levels for a certain temperature, shown in **Equation 2** below. The time necessary for a system to reach this distribution is

$$\Delta E = h\gamma B / 2\pi \quad (1)$$

$$\frac{N_d}{N_u} = e^{-h\gamma B / 2\pi kT} \quad (2)$$

represented by the value of the spin lattice relaxation time,  $T_1$ , although this value is not the full time required for relaxation.<sup>8</sup> Instead, it is more accurate to consider  $1/T_1$  as the first order rate constant for the establishment of the equilibrium described by the Boltzmann distribution.

### 1.6 $T_1$ Inversion Recovery Experiment

In order to determine the  $T_1$  for a given sample, numerous experiments have been developed. Of these, none is more accurate than the Inversion Recovery experiment, which uses a  $180^\circ$ -tau- $90^\circ$  pulse sequence. This experiment is based around the net magnetic dipole moment, known as the magnetization vector,  $\mathbf{M}_0$ , resulting from the equilibrium described by the Boltzmann distribution. When the sample is “hit” with a  $180^\circ$  pulse, the vector  $\mathbf{M}_0$  is inverted to  $-\mathbf{M}_0$ . After the initial pulse, the vector begins its spin-lattice relaxation, decreasing in negative intensity as it returns to the initial value,  $\mathbf{M}_0$ , through 0, along the z-axis. During this relaxation, after a

variable delay,  $\tau$ , the sample is again “hit”, only this time with a  $90^\circ$  pulse. This transposes the

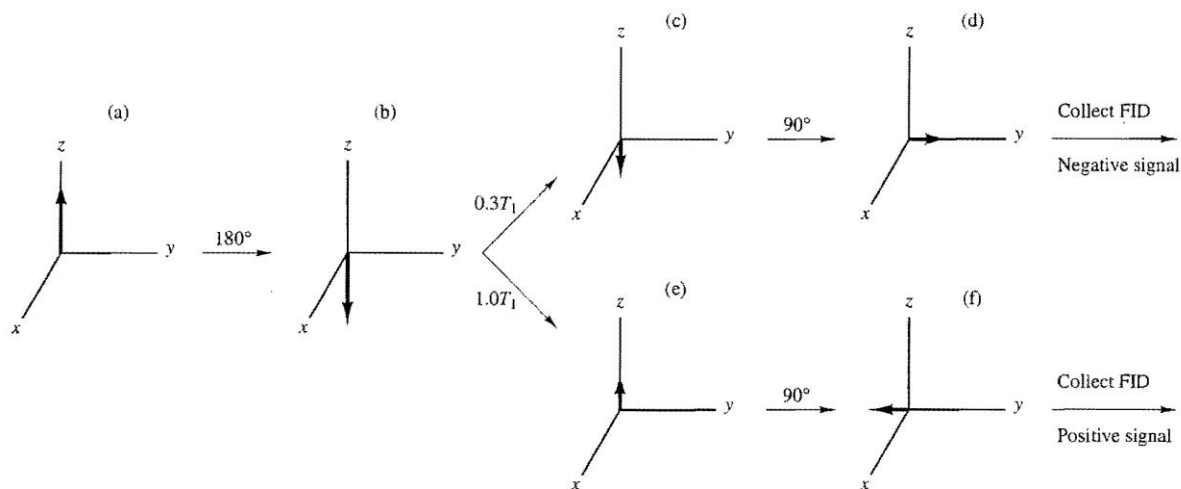


**Figure 1.** This is a vector diagram of the resulting magnetization during the pulse sequence of the  $T_1$  Inversion Recovery Experiment.<sup>8</sup>

magnetization into the transverse plane. If the delay  $\tau$  is short, the magnetization vector may still be negative, which will result in a negative intensity in the NMR spectrum. On the other hand, if  $\tau$  is longer,  $M_0$  may be either zero or positive, which would (as expected) correspond to no or a positive signal on the NMR spectrum.

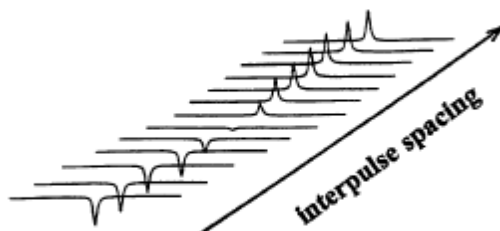


**Figure 2.** This figure shows the relationship between the interpulse spacing of the inversion recovery experiment,  $\tau$ , and the magnitude of the resulting peak.<sup>24</sup>

Once data has been collected over a range of variable delays, the relative intensities of the signal of interest can be plotted against  $\tau$ . This data may be fitted with an exponential curve according to the equation:

$$y[\tau] = \text{amp} * \left\{ 1 - \left[ 1 + \text{eff} * \left( 1 - e^{(\text{cycle time}/T_1)} \right) \right] * e^{(-\tau/T_1)} \right\} \quad (3)$$

Amp, eff, and  $T_1$  in the above equation are the empirical values calculated from the input values  $y[\tau]$  and cycle time. This fit can then be used to calculate the experimental  $T_1$  of the given sample at the given temperature. The experimental  $T_1$  values are then compared with theoretical  $T_1$  values calculated assuming various models of angular motion using the Torchia/Szabo formalism.<sup>9</sup>

### 1.7 Molecular Motion and $T_1$

Regardless of rigidity or state, all molecules are constantly undergoing some form of motion. The rate of this motion, as expected, is dependent on the amount of energy within the molecule. As this energy is increased (by raising temperature for instance), the rate of molecular motion increases. This relationship becomes important when considering the relaxation of a nucleus. Every NMR active nucleus has an intrinsic frequency at a given magnetic field, known as the Larmor frequency. The Larmor frequency,  $\omega^0$ , is proportional to the magnetic field and is given by the equation:

$$\omega^0 = -\gamma B_0 \quad (3)$$

where  $B_0$  is the magnetic field, and  $\gamma$  is the magnetogyric ratio.<sup>7</sup> As previously mentioned, there is an important relationship between this frequency and the relaxation of a nucleus, namely that the fastest possible spin-lattice relaxation occurs when the rate of molecular motion is approximately equal to the Larmor frequency. This, in turn, leads to the smallest possible value for  $T_1$ . By altering the frequency of motion within the molecule, the value of  $T_1$  will increase.

This relationship is clearly shown in Figure 3 below.

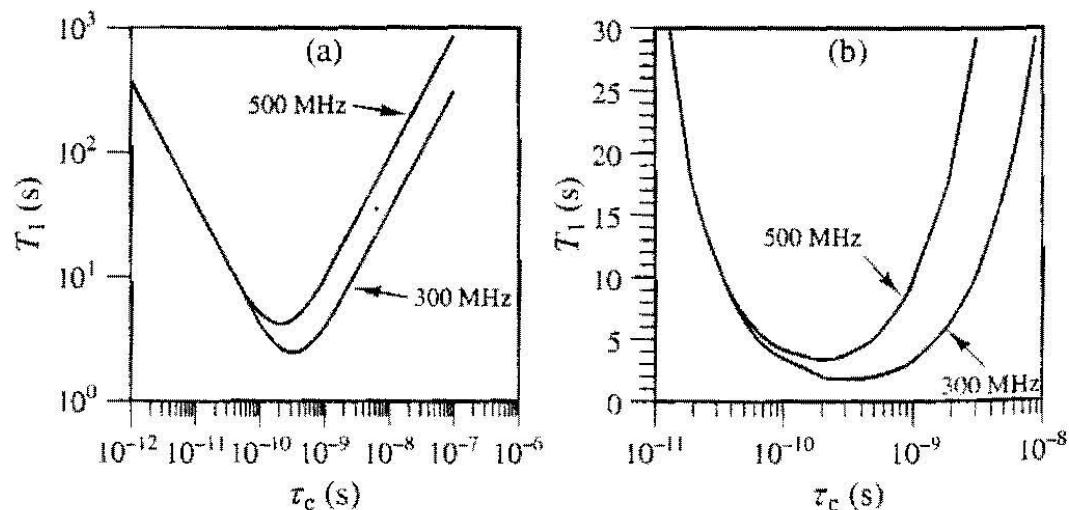


**Figure 3.** Plot of  $T_1$  versus correlation time at 7.02 T (300 MHz) and 11.75 T (500 MHz). The vertical axis in (a) is a logarithmic scale, while the same axis in (b) is linear. The latter plot covers a smaller range of values to show a better view of the convergence of the plots. It is important to note that this study plots  $T_1$  against temperature, not correlation time. While this preserves the relationship between the field strengths, it reverses the side on which they coalesce.<sup>8</sup>

### 1.8 $T_1$ Quadrupole Echo Experiment

The  $T_1$  Quadrupole Echo experiment, like its name, is basically a combination of both the Quadrupole Echo and  $T_1$  Inversion Recovery Experiments. The pulse sequence, which is again a combination of both experiments, proceeds as follows:  $180_x - \tau_1 - 90_x - \tau_2 - 90_{\pm y} - \tau_2 - \text{Acquire}$ . This sequence begins by inverting the magnetization like a typical  $T_1$  Inversion Recovery, but then follows the sequence of a Quad Echo experiment to acquire the data. By altering  $\tau_1$ , a range of quadrupole spectra with varying intensity, depending on the relaxation, can be obtained.

Much like the Quad Echo experiment is necessary to study quadrupolar nuclei in the solid state, this experiment is needed to study their solid state  $T_1$  values. This is extremely useful when studying deuterium, as relaxation in  $^2\text{H}$  is principally quadrupolar, making analysis



relatively simple. The quadrupolar interactions associated with these nuclei not only disturb their energy levels, but they also cause the spectral frequency to be angularly dependent, which in turn causes a dependence of  $T_1$  on spectral frequency.<sup>6</sup> These interactions also cause a very obvious effect on the appearance of the spectra, namely, a powder lineshape.

### 1.9 Powder Patterns and Lineshape Analysis

While NMR may appear to be strictly experimental, theoretical calculations and mathematical modeling are important aspects of this field. Arising from its dependence on the perturbation of Zeeman energy levels, which may be accurately predicted, an NMR mathematical model of any given system may be developed to simulate and produce a theoretical spectrum. Comparison to actual experimental spectra would allow for a qualitative analysis of the suitability of the fit. This process is known as lineshape analysis. A comparison between theoretical and experimental data can be seen in Figure 4.

When a sample is studied in the solid state, the isotropic averaging, which produces narrow peaks in the liquid state, is usually not present. In fact, solid-state spectra are typically complex, consisting of “powder patterns” characteristic of the detailed angular motions and rates of the motions. A large amount of information is available from these patterns. If a single crystal of a deuterated compound is analyzed in the solid state, the spectrum shows two lines, known as discrete resonances, and illustrates that separations that are exactly related to the angle between the O-D covalent bond axis and the laboratory frame. In polycrystalline samples, however, the crystals are randomly arranged in every possible orientation. The resulting resonance lineshape is the sum of the discrete pair of lines produced by each crystal due to the two allowed electronic transitions of the  $^2\text{H}$  nucleus. This line shape can be seen in Figure 5 below.

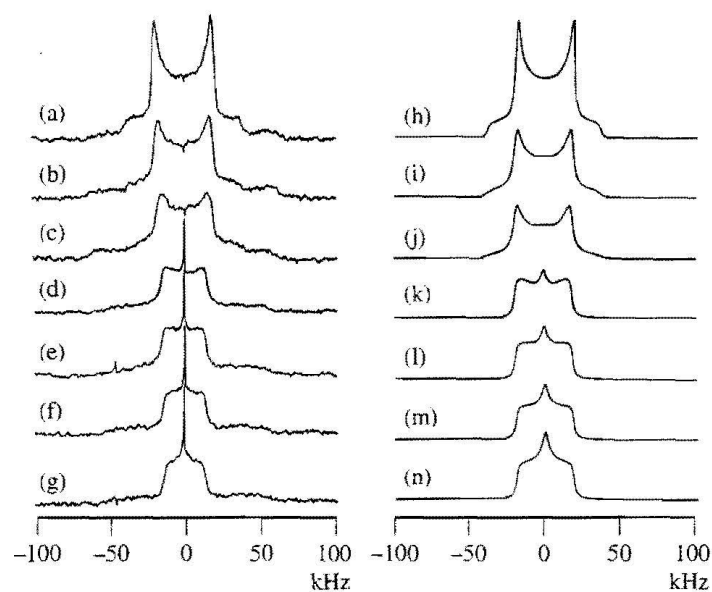


**Figure 4.** Spectra a-g Depict experimental spectra of collagen labeled with leucine-d10. Spectra h-n depict simulated spectra of the system for a C2 jump model.<sup>6</sup>

In our research, the lineshape produced by a specific molecule,  $^2\text{H}_2\text{O}$ , is of particular interest. At low temperatures, the solid state deuterium powder spectrum of  $^2\text{H}_2\text{O}$  is characterized by a quadrupole coupling constant, or qcc, of 216 kHz and an asymmetry parameter  $\eta = 0.1$ , which act as essential parameters for the simulations of various mathematical models.<sup>10</sup> Typically, if the average frequency of molecular motion is on the order of the qcc or faster, the observed frequencies are averaged and the resulting lineshape can be used to determine the angles and rate of angular motion of the O-D covalent bond. This analysis may be used to characterize this motion and differentiate between diffusion and discrete jumps.

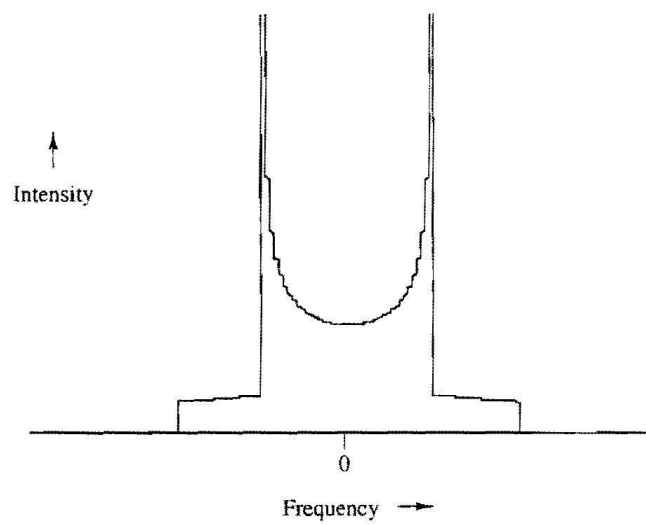


**Figure 5.** This figure shows a simulated  $^2\text{H}$  powered pattern.<sup>6</sup>

## CHAPTER TWO

### WATER

#### 2.1 Water

Covering 70% of the Earth's surface and composing over 50% of our bodies, water is the most abundant molecule on the planet. Stemming from the unique properties of water is its vital importance to all living things. Water, unlike most compounds, can be naturally found in all three states of matter. The chemical properties of this compound are of great interest to the scientific community and have been the topics of many studies. One property of particular interest for this study is the difference in molecular dynamics between the liquid and solid states.

Through its various chemical properties, water is able to form dynamic hydrogen bond networks, which are constantly changing. This is of course caused by the reorientation and motion of individual water molecules and H (D) nuclei within this network.<sup>11</sup> Because of the speed of the reorientations in the liquid state, an isotropic averaging of the dipole moments of individual molecules occurs, resulting in a single sharp peak for a particular nucleus in proton or deuterium NMR. However, water in the solid- state (ice) does not exhibit these dynamics. Although ice forms a regular lattice structure, individual O-D bonds are still able to reorient themselves within the lattice by "jumping" between allowed lattice positions. Both <sup>1</sup>H and <sup>2</sup>H NMR studies have found that "the O-H covalent bonds experience tetrahedral jumps around their molecular oxygen atom".<sup>10,12</sup> As far as several degrees below its freezing point, high symmetry tetrahedral jumps in water result in a single isotropic peak virtually identical to the liquid state peak.<sup>10</sup> At extremely low temperatures, this peak disappears and is replaced solely by the broad powder pattern expected for rigid ice.

## 2.2 The Definition of Solid State

When referring to solid-state deuterium NMR, rigidity is defined as molecular or atomic motion with a frequency substantially slower than the deuterium  $q_{cc}$  (216 kHz for  $D_2O$ ). By definition, this implies that for intervals of time shorter than  $1/q_{cc}$  the positions of the water molecules are fixed within the crystal lattice. This of course does not include small amplitude vibrations and torsional oscillations, which are present even in the most unyielding compounds. If this condition is satisfied, a rigid deuterium powder pattern is obtained. Alternatively, at higher temperatures, considerable motion starts to occur. This includes large amplitude jumps within the crystal lattice to allowed positions, which produce the narrower, characteristic deuterium powder spectra that rely on the angles and rate of motion.<sup>5</sup>

## 2.3 Solid State Tetrahedral Jumps and Bjerrum Defects

As previously mentioned, solid-state water forms a regular crystal lattice structure. The rules of this lattice structure decree that each oxygen atom should be covalently bonded to two hydrogen atoms, and that there should only be one hydrogen atom located between two oxygen atoms. As seen in Figure 6, Bjerrum defects violate these rules by either leaving two oxygen atoms with no hydrogen between them (L-defect, or Bjerrum vacancy) or leaving two hydrogen atoms occupying the oxygen-oxygen bridge (D-defect).<sup>12</sup>

Once these high energy defects are formed, they move apart instantly, causing both tetrahedral and small angle reorientations in the neighboring  $H_2O$  molecules.<sup>12</sup> Although the rate of these jumps is significantly depressed at low temperatures, they still exist at temperatures tens of degrees below water's freezing point.

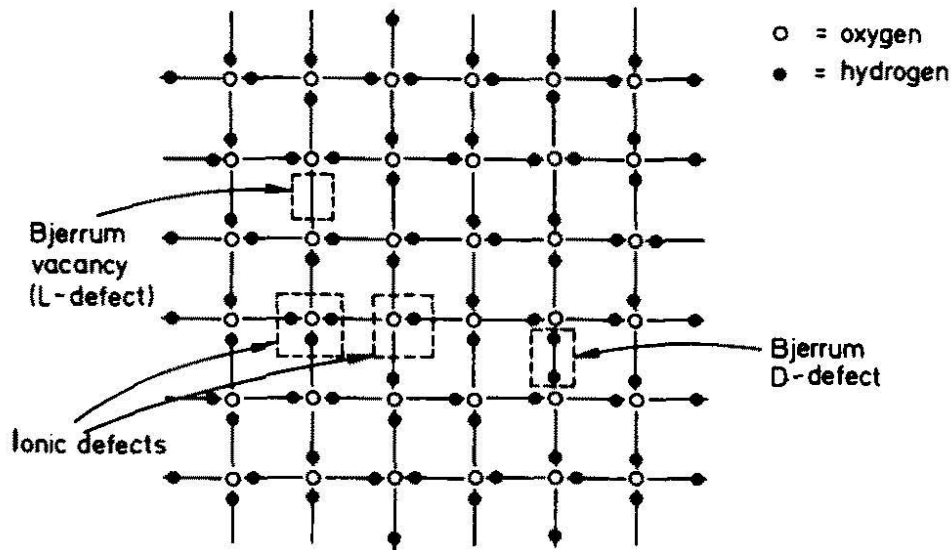


**Figure 6.** Two-dimensional slice of the tetrahedral ice lattice. The lattice of oxygen atoms is assumed to be ideal, but there are several types of defects possible in the lattice. A Bjerrum vacancy occurs when there is no hydrogen between two oxygen atoms, while a Bjerrum D-defect occurs when two hydrogen atoms are between two oxygen atoms.<sup>12</sup>

## 2.4 C<sub>2</sub> Jumps

In addition to the tetrahedral jump model for solid-state water, there have been numerous symmetrical jump models proposed in research for other systems. It is well known from observed deuterium NMR powder lineshapes of water in crystalline hydrates that the dominant water motion is C<sub>2</sub> symmetry jumps around the angle bisector of the H-O-H bonds. This essentially translates into a flip of the two hydrogen atoms without reorientation of the central oxygen atom. The O-H or O-<sup>2</sup>H bond can jump to either orientation with equal probability. However, unlike tetrahedral jumps, fast C<sub>2</sub> symmetry jumps produce a deuterium powder spectrum, not an isotropic sharp line.

## CHAPTER 3

### PREVIOUS RESEARCH

#### 3.1 Previous Studies

Several studies using deuterium NMR of  $^2\text{H}_2\text{O}$  molecules in porous solids have been carried out in our laboratory. These studies have provided undeniable evidence for the existence of solid state behavior at the melting point of water, and well above it, at atmospheric pressure. The data obtained from these studies reinforces the hypothesis that deuterated water undergoes tetrahedral jumps, in addition to  $C_2$  symmetry jumps, within the lattice of the hydrated solid.

The aforementioned studies used  $^2\text{H}$ -NMR lineshape analysis of quadrupolar echo spectra and  $T_1$  data to support this hypothesis, much like this investigation. Studies of Kanemite ( $\text{NaHSi}_2\text{O}_5 \cdot 3\text{H}_2\text{O}$ ), a simple phyllosilicate with restricted geometry,  $^2\text{H}_2\text{O}$ -hydrated  $\text{Na}^+$ -Zeolite A, and tricalcium silicate, the major component of Portland cement, have provided large amounts of evidence of solid state water participating in high symmetry jumps well above  $0^\circ\text{C}$ .<sup>13,14</sup>

Deuterium spectra collected for the  $\text{D}_2\text{O}$  in these samples were exemplified by a sharp central peak at higher temperatures like that expected for liquid  $\text{D}_2\text{O}$ , but with a  $T_1$  value almost two orders of magnitude shorter than that of liquid  $\text{D}_2\text{O}$ . This is expected for fast high symmetry jumps on a solid lattice with a jump rate comparable to the Larmor frequency. The appearance of the spectra could not solely elucidate the dynamics of the system, as the sharp central peaks could indicate liquid state  $^2\text{H}_2\text{O}$  undergoing isotropic rotation. In order to determine the origin of the central peak,  $T_1$  data was necessary. As a result,  $T_1$  inversion recovery experiments were used to determine  $T_1$  values for these peaks. Below is a table comparing experimental  $T_1$  values for Kanemite and Zeolite A along with the literature value for bulk  $^2\text{H}_2\text{O}$ .

<b>Material</b>	<b>Deuterium T<sub>1</sub> value, 46 MHz</b>	<b>Deuterium T<sub>1</sub> value, 77 MHz</b>
<sup>2</sup> H <sub>2</sub> O Synthesized Kanemite	4.6 msec	6.4 msec
<sup>2</sup> H <sub>2</sub> O Hydrated Zeolite A	7.3 msec	9.7 msec
<sup>2</sup> H <sub>2</sub> O	400 msec	400 msec

**Table 1.** Experimental deuterium spin-lattice relaxation (T<sub>1</sub>) values for Kanemite and Zeolite A and bulk isotropic liquid <sup>2</sup>H<sub>2</sub>O at 22 C.<sup>13,14</sup>

D<sub>2</sub>O in both Kanemite and Zeolite A has T<sub>1</sub> values two orders of magnitude smaller than bulk water, permitting the solid state water to be easily distinguished. Aside from the difference in T<sub>1</sub> values, T<sub>1</sub> analysis also allows for an investigation of magnetic field dependence. Both Kanemite and Zeolite A exhibit a clear dependence on the magnetic field at which the experiment is collected, while liquid water does not. This qualitative analysis demonstrates that the molecular dynamics within these solids occurs near the deuterium Larmor frequency ( $\sim 10^7$  to  $10^9$  sec<sup>-1</sup>), not comparable to the dynamics in bulk water which occur at frequencies of  $\sim 10^{11}$  to  $10^{12}$  sec<sup>-1</sup>.

### 3.2 Liquid State Isotropic Model vs. Solid State High Symmetry Model

Along with the previously mentioned inversion recovery spectra, quadrupolar echo spectra were also collected for the different porous silicates. The lineshapes of the powder patterns were analyzed against two plausible models: a liquid state isotropic model and a solid-state high-symmetry jump model. The liquid state model used is based on the dynamics of bulk water, namely high-rate isotropic rotational diffusion. Alternatively, the solid-state model was based on tetrahedral jumps equivalent to frozen water in exchange with C<sub>2</sub> symmetry jumps. The



simulation spectra were modeled according to known parameters such as the qcc and asymmetry parameters. The mathematical models were also used to calculate a  $T_1$  magnetic field dependence.

The theoretical calculations greatly favored the high symmetry jump model. Room temperature data for Kanemite and Zeolite A closely matched the theoretical calculations for the jumps.<sup>15</sup> The theoretically calculated magnetic field dependence of the  $T_1$  values is consistent exclusively with the solid-state model. All of the theoretical and experimental evidence supports the jump model, and disproves the liquid state isotropic model.

## CHAPTER FOUR

### STARCH AND CELLULOSE

#### 4.1 Introduction

Starch is a universally important compound. Not only is starch a key component in a majority of different foods, it is also the sugar storage form favored by most plants. The importance of starch for the human race becomes evident when one notes that as much as 50-70% of the energy in the human diet is derived from starch. In fact, glucose molecules obtained from the breakdown of starch are essential to brain cells, which require great deals of energy to function properly.<sup>16</sup> Starch also plays a role in food processing. During various treatments, it participates in both physical and chemical interactions with water.<sup>17</sup> The understanding of these interactions is critical to the determination of starch functionality and significance in food systems.<sup>18,19</sup>

Aside from food, starch is also used industrially. Approximately 40% of extracted starch is used for non-food purposes including pharmaceuticals, paper, adhesives, fabrics, building materials, and cement.<sup>20</sup> Much like this food, a more thorough understanding of starch's interactions with water interactions would be of great use to a number of these industrial processes.

Cellulose, unlike starch, is not digestible by humans and therefore less important in the food industry. Never the less, it is equally as useful. Cellulose is the most common organic compound on Earth and composes roughly 33% of all plant matter. It is the structural component of cell walls in green plants and some algae and is even produced by some bacteria. Cellulose holds a very important role in industry as well. It is used in the production of paper, cardboard,

and to a smaller extent cellophane, rayon, and other adhesives. It can even be used as a stationary phase in thin-layer chromatography, a common laboratory technique.

Starch and cellulose are nearly identical on a molecular level, but their structures are very different. Both polymers are made of D-glucose units. In starch, these units are connected by  $\alpha(1-4)$ -glycosidic linkages, while cellulose is connected by  $\beta(1-4)$ -glycosidic linkages (Figure 7). Starch exists in two forms: amylose and amylopectin. Both forms are made of the same linkages, but the amylose form is straight chain, while the amylopectin form is highly branched.<sup>21</sup> Typically, starch from plants consists of 80% amylopectin and only 20% amylose. Cellulose, on the other hand, has only one form. Much like amylose, cellulose forms straight chains, which form rod-like structures that are held tightly by hydrogen bonding, resulting in a high tensile strength.

Many studies have been conducted on a variety of starch's properties, including chemical, biochemical, and physical properties, functionality, and molecular structure. When studying the state of water within starch granules, NMR is clearly the technique of choice. In fact, there have been several studies which utilized NMR to investigate the distribution and state of water within starch granules.<sup>22,23</sup> Studies examining starch's interactions with water are less common, but several have made considerable progress toward understanding the various dynamics of these systems.<sup>18</sup>

Several studies focusing on the structure of starch and cellulose systems have concentrated on the interactions between the glucose monomers and water. The phenomenon of "solid-like" water adsorbed on the solids was observed in a number of these studies. Unfortunately the terminology used to describe the water differs and includes terms such as

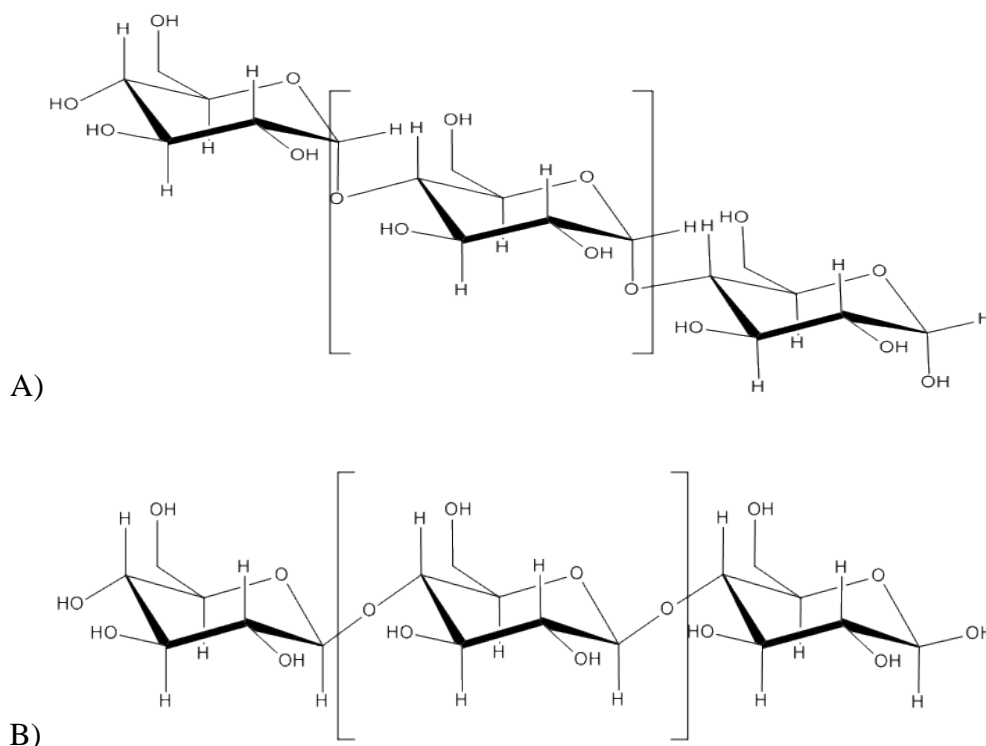


Figure 7. **The structures of starch (in the amylose form) and cellulose. A) The amylose form of starch. The amylopectin form is essentially the same, only it has regular branching. The glucose molecules of both forms of the polymer are joined by  $\alpha(1-4)$ -glycosidic linkages. B) Cellulose, unlike starch, is joined by  $\beta(1-4)$ -glycosidic linkages and exists in only one form.**

irrotational, hydrated, associated, nonfreezable, and ordered.<sup>21,24</sup> In addition to the ambiguous naming, there have also been several ways of characterizing the water into intermediate states including relatively unrestricted, semi-bulk, and tightly bound states. These states arise from multiple layers of bound water. This investigation focused mainly on the first state of tightly bound water, with low moisture content in all samples.

Previous investigations of the interactions between starch and water have indicated the presence of tightly bound water in a ratio of one water molecule per anhydroglucose unit. This result has been proven to be consistent between different starches.<sup>21</sup> X-ray experiments have suggested that the primary site of hydration is the C-6 OH group, while the C-2 and C-3 hydroxyl groups are bound to other glucose units.<sup>21</sup> The tightly bound water does not change

thermodynamically below 0°C, and although this “nonfreezable” water can reach out to three molecular layers with more extensive hydration, the first layer has been shown specifically to be “solid-like” at 20°C.<sup>21</sup> In fact, one study reported a <sup>2</sup>H NMR T<sub>1</sub> value of 8 ms at a 6% moisture content for cellulose.<sup>24</sup>

## 4.2 Experimental

### 4.2.1 Sample Preparation

All samples were placed into 5 mm NMR tubes and sealed with parafilm and epoxy to prevent atmospheric moisture uptake.

**Starch.** Deuterated starch samples were prepared by stirring native wheat starch granules (Midsol 50, MGP Ingredients, KS) into <sup>2</sup>H<sub>2</sub>O (99.9% purity, Cambridge Isotope Lab, Andover, MA) and allowing them to settle. This process was repeated three times with fresh <sup>2</sup>H<sub>2</sub>O. A slurry was then made of <sup>2</sup>H<sub>2</sub>O and starch (30% w/w) and allowed to equilibrate for two hours. Samples were then freeze-dried using a VirTis Genesis freeze drier with a 48 hour cycle under a vacuum of 300 mTorr.

**Cellulose.** Pure fibrous cellulose powder was received from Dr. Nicole Brown, School of Forest Resources. The cellulose was deuterated by creating a slurry of <sup>2</sup>H<sub>2</sub>O and cellulose powder. The mixture was sealed with parafilm and stirred for 48 hours. After mixing, the sample was freeze-dried.

#### 4.2.2 NMR Measurements

$^2\text{H}$  NMR experiments were carried out over a range of temperatures at various magnetic fields, specifically 6.98, 7.01, 7.05, 11.73, and 11.75 Tesla on five different NMR spectrometers: a solid state Tecmag-300, two different liquid state Bruker DPX-300's, a solid state Chemagnetics/Varian Infinity 500, and a liquid state Bruker AMX-2-500 at a range of carefully calibrated temperatures ( $\pm 2$  °C).

The quadrupole echo pulse sequence,  $(\pi/2)_x - \tau_1 - (\pi/2)_{\pm y} - \tau_2 - \text{Acquire}_x$  with Cyclops phase cycling added to all pulse phases and the receiver phase, was used to obtain  $^2\text{H}$  spectra on the solid state Tecmag-300 and Infinity 500 spectrometers at 45.65 and 76.77 MHz respectively ( $\pi/2 = 1.9$  to  $2.5$   $\mu\text{sec}$ ,  $\tau_1 = 30$   $\mu\text{sec}$ ,  $\tau_2 = 25$   $\mu\text{sec}$ , spectral width = 2 MHz). Variable temperature quadrupole echo spectra were obtained on solid state Tecmag-300 and Infinity 500 spectrometers using a Chemagnetics variable temperature apparatus. The temperature was calibrated with a copper constantan thermocouple taped in place inside the empty sample coil of the intact probe/variable temperature apparatus operating inside the magnet. The temperatures reported on these instruments are accurate to ca.  $\pm 2$  K over the range of temperatures investigated here. The temperatures reported on the liquid state spectrometers are accurate to  $\pm 1$  K. The experiments were conducted at temperatures ranging from  $-75$  to  $25^\circ\text{C}$ , increasing at  $25^\circ$  increments. NMR spectra were analyzed using a combination of TNMR, Spinsight and Microsoft Excel.

The  $T_1$  value of the sharp central aqueous peak was determined at various magnetic fields as a function of temperature with the inversion recovery pulse sequence,  $\pi_x - \tau_{\text{variable}} - (\pi/2)_{\phi 1} - \text{Acquire}_{\phi_{\text{ref}}}$ , with  $\phi 1 = x, y, -x, -y$  and  $\phi_{\text{ref}} = x, y, -x, -y$ , or the inversion recovery quadrupole echo experiment,  $\pi_x - \tau_{\text{variable}} - (\pi/2)_x - \tau_1 - (\pi/2)_{\pm y} - \tau_2 - \text{Acquire}_x$  (with Cyclops). At temperatures where the central peak is sufficiently sharp,  $\Delta\nu_{1/2} < 3$  kHz, the data from liquid state

spectrometers was obtained using relatively "soft" pulses a liquid state probe with  $\pi/2 \approx 13 \mu\text{sec}$  and  $\pi \approx 26 \mu\text{sec}$ . As verified by separate experiments with hard pulses ( $\pi/2 \leq 2.5 \mu\text{sec}$ ) on the solid state Tecmag-300 and Infinity-500 spectrometers, this was adequate for uniform excitation of the sharp central peak at temperatures where it could be resolved. At lower temperatures where the sharp central peak could no longer be excited with soft pulses, the  $T_1$  values were determined with  $\pi/2$  pulse widths of  $2.5 \mu\text{sec}$  or less either with the inversion recovery pulse sequence or the inversion recovery quadrupole echo pulse sequence. The measurements were taken over a wide range of temperatures from  $-25$  to  $100^\circ\text{C}$ .

### 4.3 Results and Discussion

#### 4.3.1 Quadrupole Echo Spectral Results

The quadrupole echo spectra for freeze-dried starch are shown in Figure 9. The central peak seen in the figure corresponds to the O- $^2\text{H}$  groups in the  $^2\text{H}_2\text{O}$  bound between layers of starch, while the side horns correspond to the more rigid O- $^2\text{H}$  groups of the glucose molecules. This proposed correspondence is labeled in Figure 8 for clarity.

At higher temperatures, there is a higher rate of exchange between the O- $^2\text{H}$  groups in the  $^2\text{H}_2\text{O}$  and the hydroxyl O- $^2\text{H}$  groups of glucose resulting in a sharper, better defined central peak and the inward movement of the side horns. As the temperature is decreased, the sharp central peak begins to weaken in intensity while the side horns and rigid powder pattern become more prominent as rate of exchange begins to decrease and the  $^2\text{H}_2\text{O}$  begins to freeze to yield a "rigid" powder pattern virtually identical to that of the hydroxyl groups that adds to the latter.

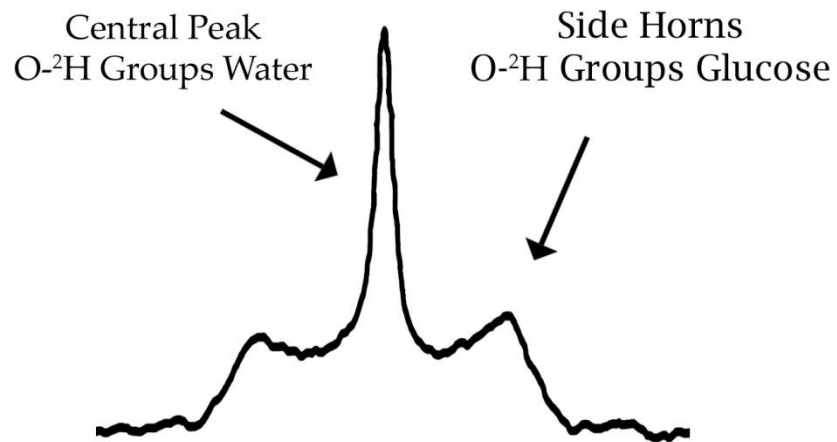


**Figure 8.** Illustration of deuterium lineshape for low-loading <sup>2</sup>H<sub>2</sub>O starch at 0°C.

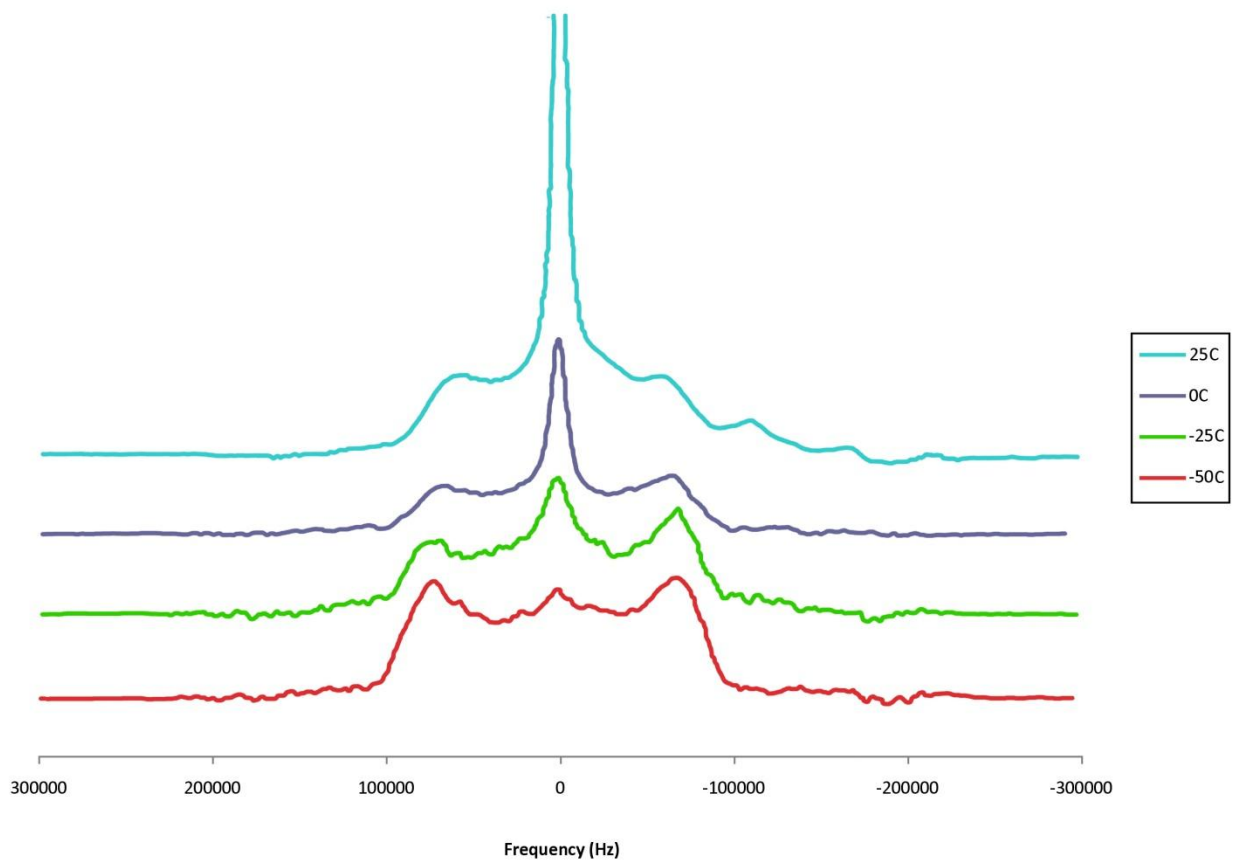


**Figure 9.** Quadrupole echo spectra for low-loading <sup>2</sup>H<sub>2</sub>O starch at -50, -25, 0, and 25°C.



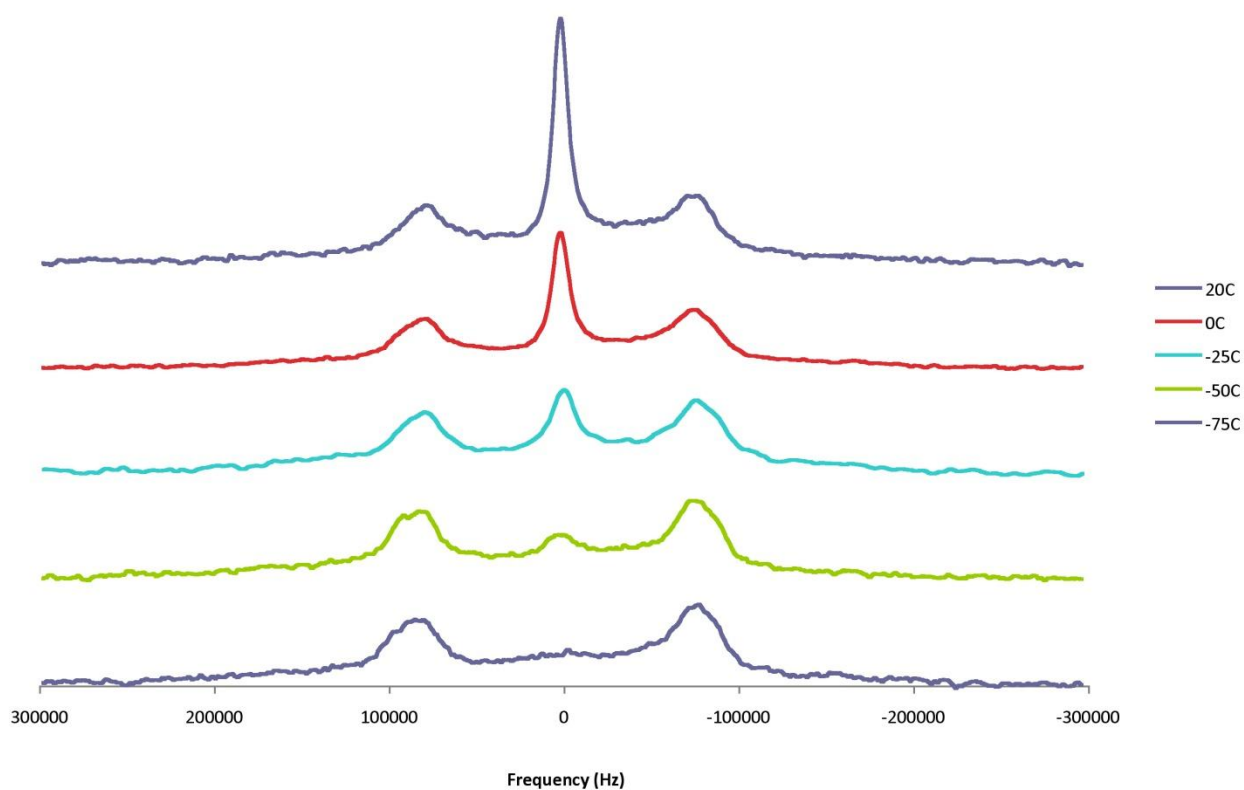


**Figure 10.** Quadrupole Echo spectra for low-loading  $^2\text{H}_2\text{O}$  cellulose at -75, -50, -25, 0, and  $20^\circ\text{C}$ .

These same trends are seen for cellulose as well (Figure 10), suggesting that a similar process occurs in both freeze dried hydrated compounds. While this similarity amounts to compelling evidence for a similar aqueous environment, these results do not give any clue as to the state of the bound water. For that determination, an analysis of experimental  $T_1$  values must be completed.

### 4.3.2 T<sub>1</sub> Inversion Recovery Results

The spin-lattice relaxation time (T<sub>1</sub>) measurements taken at a range of temperatures suggest that the bound water in both freeze dried <sup>2</sup>H<sub>2</sub>O-hydrated starch and cellulose systems is in fact in the “solid” state. The T<sub>1</sub> relaxation times for the central <sup>2</sup>H<sub>2</sub>O peak range from about 4-15 msec for starch and 5-15 msec for cellulose at 7.02 T over a temperature range from about 0-85°C. These values are comparable to those seen for solid-state D<sub>2</sub>O in Kanemite and Zeolite A and are roughly two orders of magnitude shorter than those typically seen for bulk deuterated water (~400 msec).<sup>13</sup> As demonstrated in the figures, the measured T<sub>1</sub> values appear to describe the bottom of the T<sub>1</sub> curve. These low T<sub>1</sub> times correspond to high symmetry jumps, which are not necessarily tetrahedral as seen in ice, but occur at a comparable rate to the Larmor frequency.

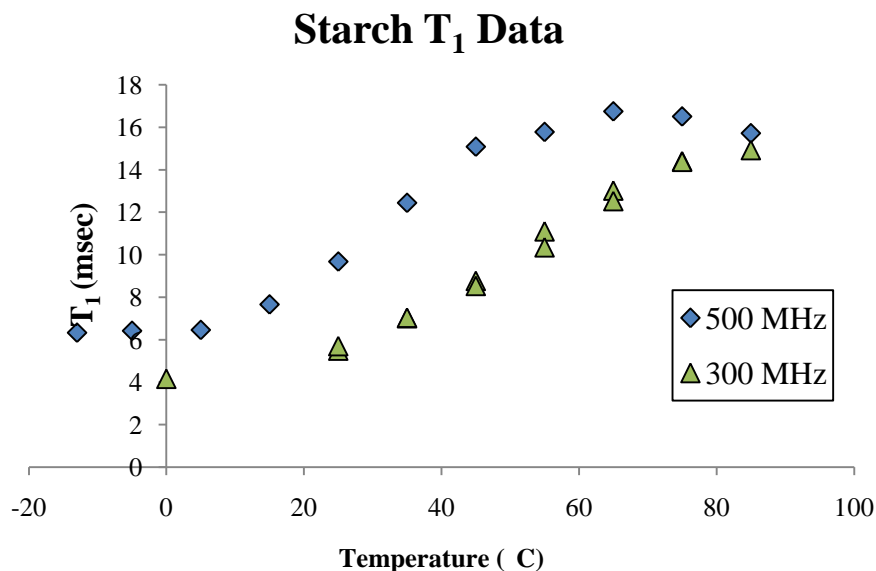


**Figure 11.** Plot of variable temperature experimental T<sub>1</sub> values for low-loading <sup>2</sup>H<sub>2</sub>O starch at 7.02 and 11.75 T.

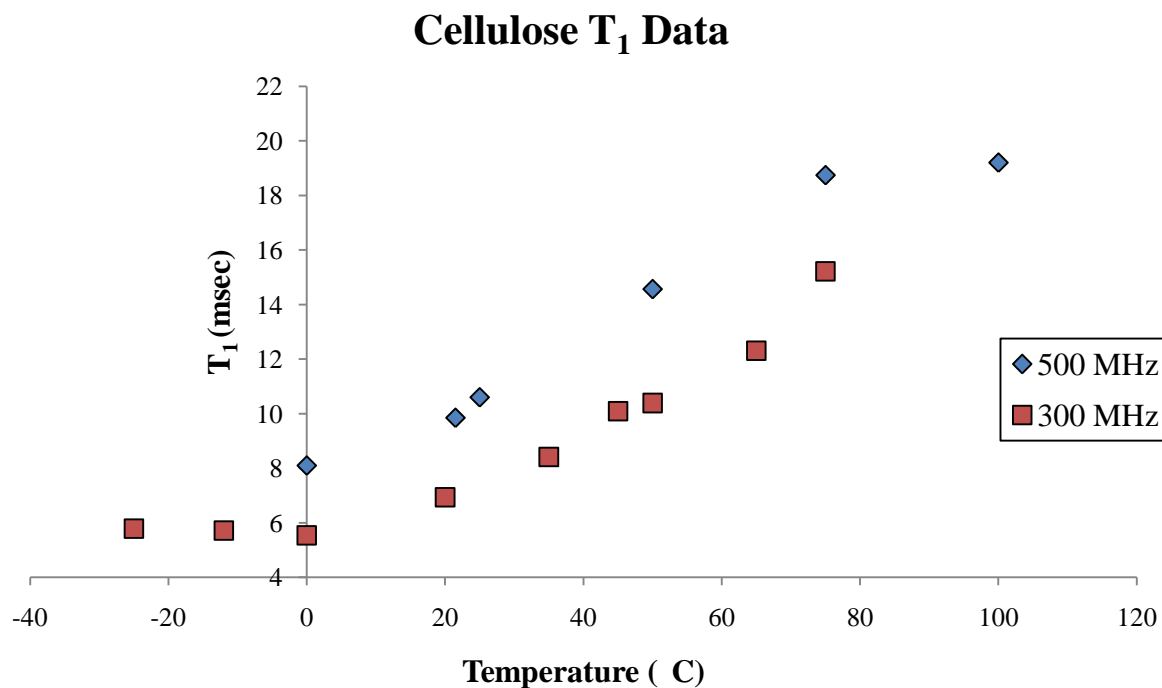


**Figure 12.** Plot of variable temperature experimental T<sub>1</sub> values for low-loading <sup>2</sup>H<sub>2</sub>O cellulose at 7.02 and 11.75 T.

This result suggests that the water is in the solid state because in the temperature range used in this study, only solids have been known to move at this frequency. Furthermore, because of the order inherent in most solids, only high symmetry jumps such as tetrahedral and C<sub>2</sub> have been seen in this state.

T<sub>1</sub> data was collected on both solid state and liquid state spectrometers at 7.02 and 11.75 T (300 and 500 MHz). The T<sub>1</sub> values measured on each instrument of identical field strength were found to be identical within experimental error, which signified the reproducibility of these results. The T<sub>1</sub> values obtained from the solid and liquid-state instruments were combined for each magnetic field to produce one curve. In both the starch and cellulose data, there is clearly a dependence on the magnetic field, with the higher magnetic field producing higher T<sub>1</sub> values.

As seen in Figures 11 and 12, higher temperatures, specifically those collected on 11.75 T (500 MHz) spectrometers, show a slight leveling off of the curve and a depression of the  $T_1$  values. It is hypothesized that this trend is caused by an exchange between the deuterons of the central peak and the deuterons of the hydroxyl groups. At higher temperatures, an increased mobility allows for deuteron exchange between the jumping water molecules, and the less mobile O- $^2\text{H}$  groups of the glucose rings. The  $T_1$  values of the mobile groups are decreasing at a rate faster than the rate at which the  $T_1$  values of the water molecules are increasing. The exchange between these groups causes each group to impart some of its “character” to the other, thereby lowering the  $T_1$  of the central peak and also shifting the horns towards the central peak. This final result is best seen in Figures 9 and 10 of section 4.3.2.

#### **4.4 Conclusions and Future Research**

$^2\text{H}$  quadrupolar echo and  $T_1$  inversion recovery experiments were conducted on starch and cellulose samples at two magnetic fields, covering a wide range of temperatures on both liquid and solid state spectrometers. The experimental data is consistent with previous research within this group on porous silicates. It is, in fact, in support of a hypothesis for the existence of solid-state, tightly bound surface water. These results are also consistent with other studies on the dynamics of water within starch and cellulose systems. Both deuterium lineshapes and  $T_1$  values suggest that the  $^2\text{H}$  nuclei in low loading  $^2\text{H}_2\text{O}$  starch and cellulose samples experience high-symmetry jumps similar to those observed in  $^2\text{H}_2\text{O}$  ice,  $^2\text{H}_2\text{O}$ -synthesized Kanemite, and  $^2\text{H}_2\text{O}$ -hydrated Zeolite A. Another proposed hypothesis, that the surface water within these samples remains in the liquid state above the freezing point, is not supported by the experimental  $T_1$  data.

In order to verify the qualitative conclusions of this study, a new jump model must be developed in order to compare simulated data with collected data. While it is possible that the previous C<sub>2</sub>/Tetrahedral jump model could apply for these systems, it is more likely that the basic structural differences between porous silicates and polymeric glucose chains would result in somewhat different dynamics. The interactions between the water and the surface groups of the various glucose chains would have to be further studied in order to create an accurate model.

A continuation of this study should be to further explore aqueous dynamics in these and other systems. It is possible that similar solid-state hydrated systems are common and therefore important to a variety of scientific fields. In particular, hydrogen fuel cell membranes such as Nafion are suspected to contain similar structures. A further exploration into the dynamics of such systems could lead to better understanding of proton transfer and aid in the design of more effective membranes.

## REFERENCES

1. I.I. Rabi, J.R. Zacharias, S. Millman, P. Kusch (1938). A New Method of Measuring Nuclear Magnetic Moment. *Phys. Rev.* **53**: 318
2. Bloch, F. Nuclear induction. *Phys. Rev.* **1946**, *70*, 460-473.
3. Bloch, F.; Hansen, W.W.; Packard, M. Nuclear induction, *Phys. Rev.* **1946**, *69*, 127.
4. Quadrupolar Nuclei in Solids. *Encyclopedia of Nuclear Magnetic Resonance*, 2<sup>nd</sup> ed.; John Wiley: New York, 1996; pp 3869-3884.
5. Phair, J.W.; Livingston, R.A.; Brown, C.M.; Benesi, A.J. Investigation of the State of Water in Hydrating Layered Sodium Disilicate in Crystalline and Amorphous Forms by Quasi-Elastic Neutron Scattering. *Chem. Mater.* **2004**, *16*, 5042.
6. Deuterium NMR in Solids. *Encyclopedia of Nuclear Magnetic Resonance*, 2<sup>nd</sup> ed.; John Wiley: New York, 1996; pp 1547-1581.
7. Levitt, M.H. *Spin Dynamics: Basic of Nuclear Magnetic Resonance*; John Wiley & Sons, Ltd.: New York, 2001.
8. Relaxation: An Introduction. *Encyclopedia of Nuclear Magnetic Resonance*, 2<sup>nd</sup> ed.; John Wiley: New York, 1996; pp 3988-4002.
9. Torchia, D.A.; Szabo, A. Spin-lattice relaxation in solids, *J. Magn. Res.* **1982**, *49*, 107-121.
10. Wittebort, R.J.; Usha, M.G.; Ruben, D.J.; Wemmer, D.E.; Pines, A. Observation of Molecular Reorientation in Ice by Proton and Deuterium Magnetic Resonance. *J. Am. Chem. Soc.* **1988**, *110*, 5668.
11. Laage, D.; Hynes, J.T. A molecular jump mechanism of water reorientation. *Science*, **2006**, *311*, 832-835.

12. Fujara, F.; Wefing, S.; Kuhs, W.F. Direct Observation of Tetrahedral Hydrogen Jumps in Ice Ih. *J. Chem. Phys.* **1988**, *88*, 6801.
13. Benesi, A.J.; Grutzeck, M.W.; O'Hare, B.; Phair, J.W. Room-Temperature Icelike Water in Kanemite Detected by  $^2\text{H}$  NMR  $T_1$  Relaxation. *Langmuir*. **2005**, *21*, 527.
14. O'Hare, B.; Grutzeck, M.W.; Kim, S.G.; Asay, D.B.; Benesi, A.J. Solid State Water Motions Revealed by Deuterium Relaxation in  $^2\text{H}_2\text{O}$  -Synthesized Kanemite and  $^2\text{H}_2\text{O}$  -Hydrated  $\text{Na}^+$ -Zeolite A. *J. Mag. Res.* **2008**, *195*, 85.
15. Benesi, A.J.; Grutzeck, M.W.; O'Hare, B.; Phair, J.W. Room Temperature Solid Surface Water with Tetrahedral Jumps of  $^2\text{H}$  Nuclei Detected in  $^2\text{H}_2\text{O}$ -Hydrated Porous Silicates. *J. Chem. Phys. B.* **2004**, *108*, 17783.
16. Copeland, L.; Blazek, J.; Salman, H.; Tang, M.C. Form and Functionality of Starch. *Food Hydrocolloids*. **2009**, *23*, 1527-1534.
17. Chatakanonda, P.; Dickinson, L. C.; Chinachoti, P. Mobility and distribution of water in cassava and potato starches by  $^1\text{H}$  and  $^2\text{H}$  NMR. **2003**, *J. Agric. Food Chem*, *51*, 7445-7449.
18. Tananuwong, K.; Reid, D. S. Differential scanning calorimetry study of glass transition in frozen starch gels. **2004**, *J. Agric. Food Chem.*, *52*, 4308-4317.
19. Choi, S.G.; Kerr, W.L.  $^1\text{H}$  NMR studies of molecular mobility in wheat starch. **2003**, *Food Research Intl.*, *36*, 341-348.
20. Burrell, M.M. Starch: the need for improved quality and quantity – an overview. *J. Exp. Bot.*, **2003**, *54*, 451–456.
21. Zografi, G.; Kontny, M.J. The interactions of water with cellulose- and starch-derived pharmaceutical excipients. *Pharm. Res.*, **1986**, *3*, 187-194.

22. Tang, H. R.; Godward, J.; Hills, B. The distribution of water in native starch granules—a multinuclear NMR study. *Carbohydr. Polym.* **2000**, *43*, 375-387.
23. Botlan, D. L.; Rugraff, Y.; Martin, C.; Colonna, P. Quantitative Determination of Bound Water in Wheat Starch by Time Domain NMR Spectroscopy. *Carbohydr. Res.* **1998**, *308*, 29-36.
24. Vittadini, E.; Dickinson, L.C.; Chinachoti, P.  $^1\text{H}$  and  $^2\text{H}$  NMR mobility in cellulose. *Carbohydr. Polym.* **2001**, *46*, 49-57.



## Academic Vita

### Sasha Slipak

Permanent Address: 7 Moloney Drive  
Tannersville, PA 18372  
Cell: (570) 856-1558

Local Address: 219 Waupelani Dr. Apt W-07  
State College, PA 16801

### EDUCATION

**The Pennsylvania State University**, University Park, PA

Bachelors of Science in Chemistry

Bachelors of Science in Mathematics

#### Honors and Awards:

Schreyer Honors Scholar

Spring 2010 Marshal of Chemistry

Bayard D. Kunkle Scholarship, Meyer Fleming Analytical Chemistry Award, and Teas  
Scholarship recipient

#### Relevant Coursework:

Basic and Advanced Organic Chemistry Laboratory

Physical and Analytic Chemistry Laboratory

### LABORATORY EXPERIENCE

- Proficient at various synthetic and purification techniques
- Skilled at operating and interpreting various analytical instruments including: NMR, IR, GC, GC-MS, and Differential Scanning Calorimeters.
- **Undergraduate Research**  
**NMR Spectroscopy with Dr. Alan Benesi (January 2008- Present)**
  - Run experiments on solid and liquid state NMR spectrometers
  - Analyze spectrums from a variety of experiments
  - Tune NMR probes for different target nuclei
  - Completed Chemical and Hazardous Waste training course

### WORK EXPERIENCE

- **Chemistry Undergraduate Teaching Asst. – The Pennsylvania State University (2010-Present)**
  - Teach students various organic laboratory techniques
  - Assist students with using various analytical instruments
  - Help students to interpret various analytical spectra
- **Biology Undergraduate Teaching Asst. – The Pennsylvania State University (2008-2009)**
  - Assisted students with performing biological laboratory techniques and experiments
  - Facilitated communications between a foreign Teaching Assistant and students
  - Helped set up experiments and laboratory equipment
  - Explained various biological concepts to students

### LEADERSHIP EXPERIENCE

- Science LionPride Executive Founding Webmaster August 2008-Present, President October 2009-Present
- Penn State Math Club 2006-Present, Treasurer(2008-2009), Vice President (2009-2010)
- Member of the Penn State Pre-Medical Preceptorship Program Summer 2008
  - Observed Physicians in a variety of medical fields over a one month period
- Independent Math and Chemistry Tutor Spring 2007-Present
- Nittany Chemical Society Webmaster 2009-Present

### SKILLS

- Literate Microsoft Office, Windows, Linux, C++
- Russian – Read and speak fluently